

Mechanism of the ozone formations in a near liquid nitrogen temperature medium pressure glow discharge positive column

Jen-Shih Chang* and S. Masuda**

Department of Electrical Engineering, The University of Tokyo, Tokyo, Japan

*On leave from Dept. of Eng. Phys., McMaster University, Hamilton, Ontario, Canada L8S 4M1

** Present address Fukui Institute of Technology Fukui, 910 Japan and Masuda Research Inc. Tokyo, 113 Japan

Abstract - Mechanism of the ozone formations in a near liquid nitrogen temperature medium pressure DC glow discharge positive column has been proposed, and numerical and experimental investigations have been conducted.

INTRODUCTION

Production of ozone by medium pressure glow discharge has been attempted by many authors and review has been given by Horvath [1]. Briner et al [3] observed that the temperature in the discharge space from 293[K] to between 203 and 193 [K] increases the ozone production to 2.3-fold when oxygen is used. Throp et al [2] used liquid nitrogen cooling glow discharge ozone generators, and 40 to 45[%] the conversion of oxygen at the energy yield 300 [g/KWh] was obtained. More recently Masuda et al [4] confirmed these results and up to 580 [g/KWh] energy yield was obtained. In this work, mechanism of the ozone formations in a near liquid near nitrogen temperature medium pressure glow discharge positive column plasma is proposed and some numerical results are presented for pure oxygen discharges.

PLASMA CHEMISTRY AND BASIC EQUATIONS

Overall plasma chemistry for oxygen discharge is shown in Figure 1, where all reaction rates from the review of the references [5-7] and units are [cm³/s] for two body and [cm⁶/s] for the three body reactions. Negative ions in the system are O⁻, O₂⁻, O₃⁻ and O₄⁻ and the positive ions are O⁺, O₂⁺, O₄⁺ and O₆⁺. The radial and metastable species are O, O*, O₂^{*}, O₃ and O₆, i.e. O* represents O(1D), O(1S) and O(3P), and O₂^{*} represents O₂(a¹Δg), O₂(1Σg⁺).

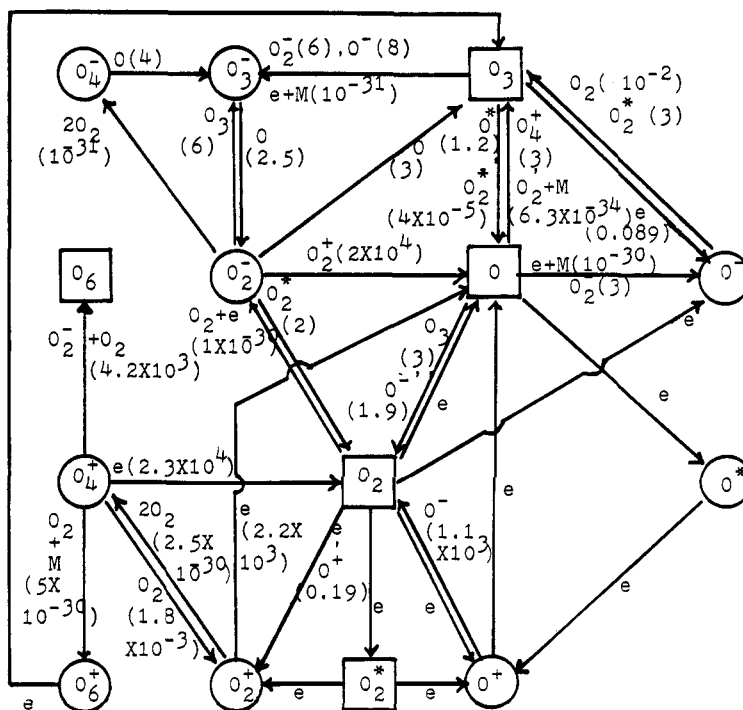
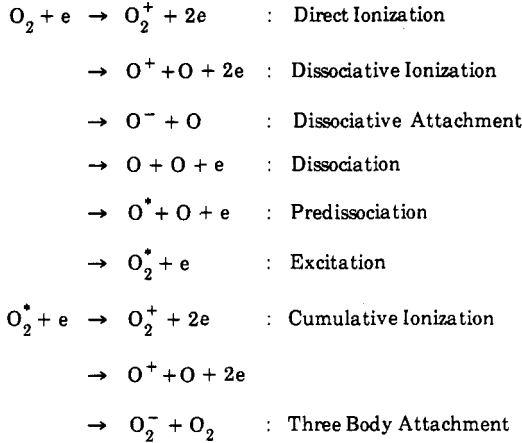
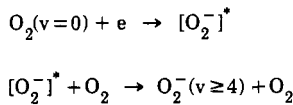


Fig. 1 Plasma chemistry for oxygen discharges: × 10⁻¹⁰ [cm³/s] for two body, [cm⁶/s] for three body reactions.

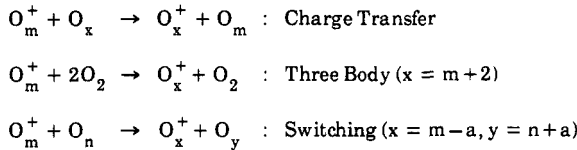
Plasma will be initiated by electrons with reactions as follows:



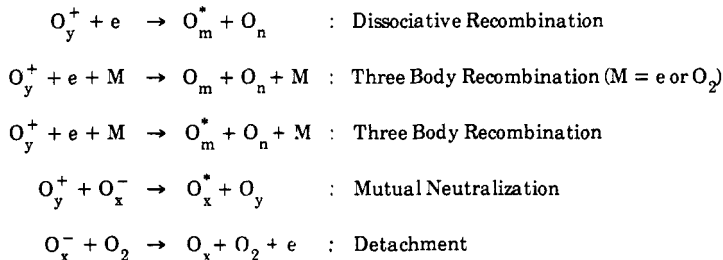
Fraction of dissociative ionization cross section is approximately below 10 [%] of total ionization cross section (ref. 11) in the present range of electron temperature (≤ 3 [eV]), and no significant influence of gas temperature was observed (ref. 12). Direct attachment reaction $\text{O}_2 + e \rightarrow \text{O}_2^- + hv$ is the the order of 10^{-19} [cm³/s] at 300 [K]. However, this reaction becomes important when gas pressure becomes higher due to the collisional detachment reaction (ref. 13) as follows:



where we must note that the reaction becomes significantly influenced by gas and electron temperatures, since vibrational state is involved (see Table 1). Similar reactions will occur for the produced neutral species O and O₃. O_y⁺ and O_x⁻ ions are usually produced through the ion-molecule as follows:



where m, n, a, x, y = 1 to 6 and similar reactions can occur for negative ions. The loss process of these ions are the detachment, mutual neutralization, three body and dissociative recombinations as follows:



From these fundamental processes, we can observe that the free radical species such as O and O₃ can be produced not only from the direct processes, but also from the electronic and ionic processes. Under the medium gas pressure range considered in the present work, the degree of the ionization is in between 10^{-2} - 10^{-6} [%]. However, the order of two body reaction rate related electron or ion species is 10 to 10^8 times large, compared with neutral reactions, i.e. the reaction rate $k \approx 10^{-6}$ - 10^{-8} for electronic, $k = 10^{-9}$ - 10^{-12} for ionic and $k \approx 10^{-11}$ - 10^{-17} for neutral reactions. Therefore, the effective production or loss rate of each species becomes comparable for ionic and neutral processes, since the rate equation is

$$\begin{aligned}
 \frac{d[X]}{dt} &= (\text{reaction rate}) \times (\text{density of reactant}) \times [X] && \text{or} \\
 &= (\text{reaction rate}) \times (\text{density of reactant A}) \times (\text{density of reactant B})
 \end{aligned}$$

for species X, where [X] indicates density of species X.

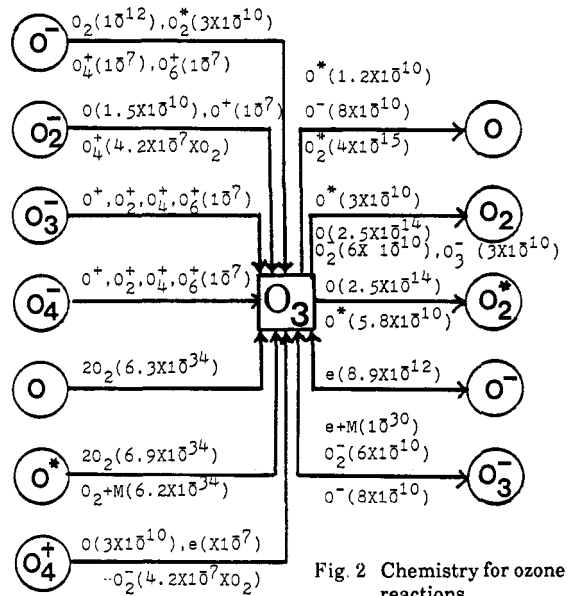


Fig. 2 Chemistry for ozone reactions.

If we only focus on the ozone formations, the ozone production and loss processes are summarized in Figure 2. The ozone formation can be achieved from the ion-molecule reaction of the positive and negative ions, and three body reactions of oxygen atoms. However, free radical oxygen atoms also act as a major loss process to the ozone. Figures 1 and 2 show that the equilibrium ozone density is function of the electric field (or electron temperature), gas temperature, pressure and plasma density (or discharge power). Gas and electron temperature dependences of reaction rates obtained from references (5-7) are summarized in Table 1.

A method to estimate plasma parameters, ion and free radical compositions for the medium pressure positive column plasma in which various chemical reactions occur has been developed by Ichikawa et al. (refs. 8, 9). This method was modified to calculate the gas temperature dependence of oxygen discharge (computer code: OPPC, ref. 14). The coupled governing equations for each ion and free radical species can be expressed as follows:

$$D_k \nabla^2 N_k + (\text{source})_k - (\text{sink})_k = 0$$

where N_k is the number density of species k and D_k is the ambipolar diffusion coefficient for ion species k or diffusion coefficient of free radical particles k . Basic properties of ozone and oxygen is shown in Table 2. Table 2 shows that ozone will be an ice or liquid forms near liquid nitrogen temperatures. This condition will effect diffusion of ozone particles, and lumped in net diffusion coefficients in the present model, i.e. adding thermophoresis and diffusiphoresis effects (ref. 10).

Gas temperature dependence of reaction rates shown in Table 1 are extrapolated up to the 100 [K] in the present work.

Table I Gas temperature dependence of reaction rates

	Reactions	Temperature Dependence	Temperature Range (K)
Radical Reactions	$O + 2O_2 \rightarrow O_3 + O_2$	$2.5 \times 10^{35} \exp(970/T)$	220-370
	$O + O + M \rightarrow O_2 + M$	$1.3 \times 10^{32} (T/300)^1 \exp(-170/T)$	1000-8000
	$O^* + 2O_2 \rightarrow O_2 + O_3$	$6.9 \times 10^{-34} (T/300)^2$	
	$O_3 + O^* \rightarrow 2O_2$	$1.5 \times 10^{-11} \exp(-2218/T)$	200-1000
	$O_3 + O_2^* \rightarrow O + 2O_2$	$1.2 \times 10^{-11} \exp(-2400/T)$	200-1000
Ion-Molecule Reactions	$O^- + O_2 + M \rightarrow O_3^- + M$	$1.1 \times 10^{-30} (T/300)^{-1}$	
	$O^+ + O_2 \rightarrow O_2^+ + O$	$2 \times 10^{-11} (T/300)^{-0.5}$	
	$O_2^+ + 2O_2 \rightarrow O_4^+ + O_2$	$4 \times 10^{-30} (T/300)^{-2.93}$	40-400
Ion-Ion Recombinations	$O_x^- + O_y^+ \rightarrow O_m^* + O_n$	$A \times 10^{-7} (T/300)^{-0.5}$	
	$O_x^- + O_y^+ + M \rightarrow O_m^* + O_n$	$B \times 10^{-25} (T/300)^{-2.5}$	
Electron-Ion Recombinations	$O_y^+ + e \rightarrow O_m^* + O_n$	$C \times 10^{-7} (T/300)^{-0.6}$	200-600, $T_{e,g}$
	$O_y^+ + e + M \rightarrow O_m^* + O_n + M$	$D \times 10^{-26} (T/300)^0$	
	$O_v^+ + e + e \rightarrow O_m^* + O_n + e$	$E \times 10^{-29} (T/300)^{-4.5}$	
Detachment	$O_2^- + O_2 \rightarrow O_2 + O_2 + e$	$2.7 \times 10^{-10} (T/300)^{0.5} \exp(-5590/T)$	
Attachment	$O + e \rightarrow O^- + h$	$1.3 \times 10^{-15} (T/300)^0$	150-500
	$O + e + M \rightarrow O^+ + M$	$1 \times 10^{-31} \exp(300/T)$	
	$O_2 + e + O_2 \rightarrow O_2^- + O_2$	$2.2 \times 10^{-29} (300/T)^{1.5} \exp(-900/T)$	195-600
	$O_3 + e \rightarrow O^- + O_2$	$8.9 \times 10^{-12} (T/300)^{1.5}$ or $1.9 \times 10^{-9} T_e^{-1.45}$	0.02-0.5 (eV)

Table II Basic property of Oxygen and Ozone

	Melting point	Boiling point	Density-Liquid	-Gas
Oxygen	54.8 (K)	90.19(K)	1.28 (g/cm ³)	1.43 (Kg/m ³)
Ozone	80.2+ 0.5	161.3+0.3	1.61	2.14

NUMERICAL RESULTS

Typical discharge tube radius, plasma density, gas temperature and gas pressure dependences of the ozone density inside center of positive column are shown in Figures 3, 4, 5 and 6 respectively. Figure 3 shows that the ozone density has a nonmonotonic dependence to the discharge tube radius, since electron temperature (or axial electric field) is significantly influenced by a tube radius. However, the optimum ozone production condition in terms of tube radius must be carefully investigated, since ozone particle deposition rate to the cold wall is also function of the tube radius. Figure 4 shows that the ozone density decreases with increasing plasma density (or discharge power) and increases with increasing gas pressure. Figures 5 and 6 show that ozone density increases with decreasing gas temperature and the effect of gas pressure becomes more complex under lower gas temperatures, since as summarized in Table 3, major reactions for ozone at gas temperature 165 and 300 [°K] significantly different each others under these conditions. In the gas temperature below 170 [°K], no direct ion or electron related reactions are involved in ozone production and loss processes, ozone density can be approximated by simple equations

$$[O_3] = \frac{k_1 [O][O_2]^2}{k_2 [O]} = \frac{k_1}{k_2} [O_2]^2$$

where

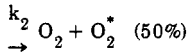
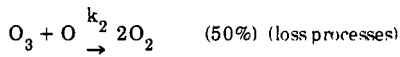


Table III Major reactions for ozone at gas temperature 165 and 300 (K).

	300 (K)	165(K)
Production Reactions	1. $O + 2O_2 \rightarrow O_3 + O_2$	same
	2. $O^- + O_2^* \rightarrow O_3 + e$	same
	3. $O_4^+ + O \rightarrow O_3 + O_2^+$	same
	4. $O^- + O_2 \rightarrow O_3 + e$	same
	5. (-)	$O_4^+ + e \rightarrow O_3 + O^*$
Loss Processes	1. $O_3 + O \rightarrow O_2 + O_2$ or O_2^*	same
	2. $O_3 + O^- \rightarrow O_2 + O_2 + O$	(-)
	3. $O_3 + O^- \rightarrow O_3^- + O$	same
	4. $O_3 + O_3^- \rightarrow 3O_2 + e$	same

This fact can be observed more clearly from Figure 7, where relative concentration of the ion and neutral species for gas temperature at 165 and 300 [K] are compared in this figure. Figure 7 shows that free radical oxygen atom density decreases with increasing ozone density, while excited oxygen molecules increase. Figure 7 also shows that relative concentration of the ion species is significantly influenced by gas temperatures and these influences significantly contribute ozone density as shown in Table 3.

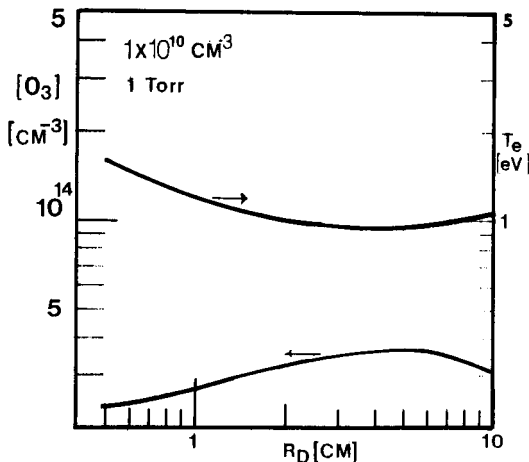


Fig. 3 Ozone density and electron temperature as a function of tube radius

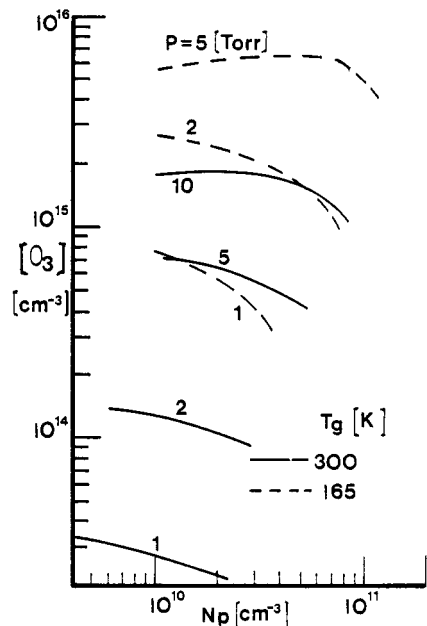


Fig. 4 Ozone density at center of discharge tube as a function of plasma density for various gas pressures and temperatures for 1.6 [cm] I.D. discharge tubes.

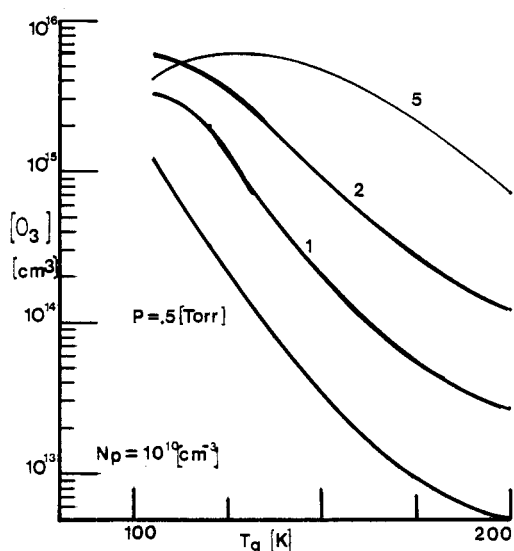


Fig. 5 Ozone density as a function of gas temperature for various gas pressures for 1.6 [cm] I.D. tubes at plasma density 10^{10} [cm⁻³].

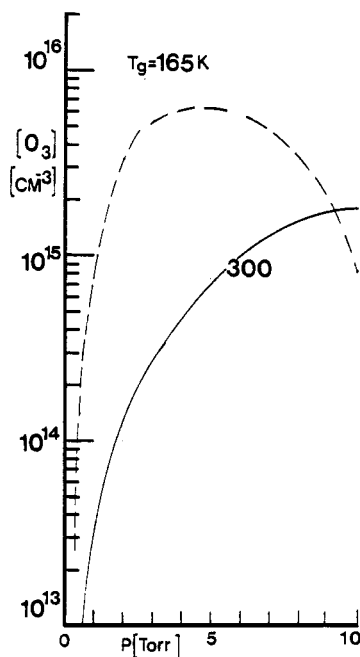


Fig. 6 Ozone density as a function of a gas pressure for various gas temperatures for 1.6 [cm] I.D. tubes at plasma density 10^{10} [cm⁻³].

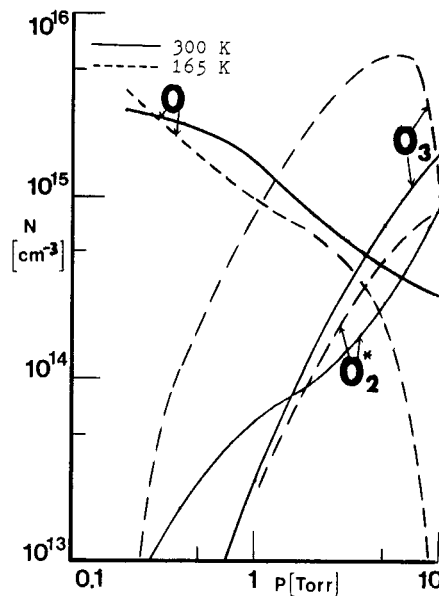
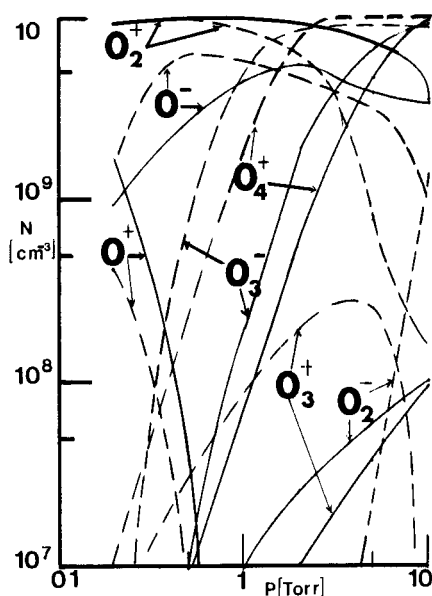


Fig. 7 Relative concentration of the ion and neutral species for gas temperature at 165 and 300 [K] for 1.6 [cm] I.D. discharge tubes at plasma density 1.2×10^{10} [cm⁻³].

EXPERIMENTAL CONFIRMATION

Experimental confirmations have been conducted by using 16 [mm] I.D. tube with DC and Ring type 13.75 [MHz] RF discharges. The shape of discharge tube used is similar to those used by Thorp et al (ref. 2) and Masuda et al (ref. 4) except oxygen is pre-cooled by liquid nitrogen as well as discharge sections. The amount of ozone produced are determined by the collected liquid ozone. Typical ozone energy yield as a function of discharge power and gas pressure is shown in Figures 8 and 9, respectively. Numerical results by assuming 10^{10} [cm⁻³] plasma density at 35 [W] and linear proportional to the discharge power is shown in Figure 8, where plasma density is also assumed to be not influenced by gas pressure changes for fixed discharge powers. Figures 8 and 9 show that an ozone production increases with increasing gas pressures and decreasing discharge powers, and present model predict these efficiencies relatively well except relatively low gas pressures ($p < 0.5$ [Torr]) and larger discharge power ($W > 10$ [w]). The discrepancy may be due to the inadequate analyses of ozone scavenging effect treatment through diffusion models, since ozone may homogeneously nucleate under these temperatures (estimated $T_g \approx 110$ [K]).

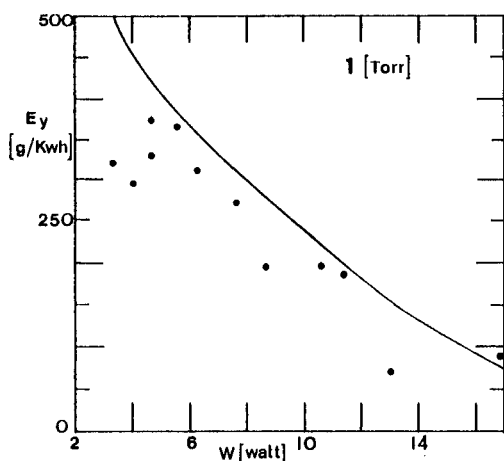


Fig. 8 Ozone energy yield as a function of discharge power; -- theory, o o o experiment.

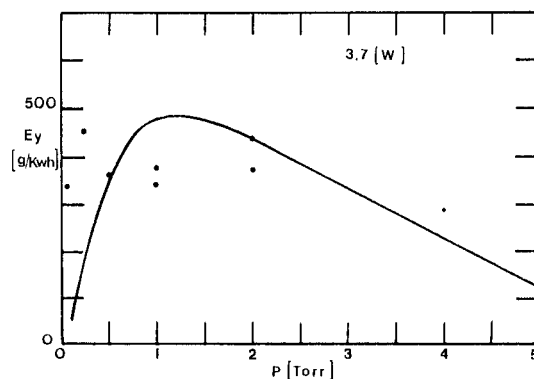


Fig. 9 Ozone energy yield as a function of gas pressure; -- theory, o o o experiment

CONCLUDING REMARKS

Mechanism of the ozone formations in a near liquid nitrogen temperature medium pressure glow discharge positive column plasma has been proposed and following concluding remarks are obtained: (1) ozone production rates are significantly influenced by reactor tube radius, gas temperatures, gas pressures and discharge powers. Optimization can be conducted by present computer codes; (2) No direct ion or electron related processes is involved near liquid nitrogen temperature ozone formations while direct ionic processes can not neglected in room temperatures; (3) An ozone production efficiency increases with increasing gas pressure and decreasing discharge power, and the energy yield as high as 600 [g/kWh] is observed from experiments. These results agree well with present numerical predictions.

Acknowledgements

The authors wish to express their appreciation to Y. Ichikawa, S. Ono, B. Eliasson, and V. Kogelschatz for valuable discussions and comments. This work was partly supported by the Natural Sciences and Engineering Research Council of Canada (JSC).

REFERENCES

- [1] M. Horvath, "Ozone" Akadémiai Kiado, Budapest (with Elsevier Sci. Pub. Co.), Ch. 3 (1985).
- [2] C.E. Thorp, L.C. Kinney and A.J. Gaynor (Air Reduction Co. Inc.) "Ozone Manufacture", Canadian Patent No. 570915 (1955/1959).
- [3] E. Briner, R. Patry and E. de Luserma, *Helv. Chim. Acta*, **7**, (1924).
- [4] S. Masuda, S. Koizumi, J. Inove and H. Arkai, *Conf. Record of IEEE/IAS meeting* (1986).
- [5] B. Eliasson and V. Kogelschatz, Brown Boveri Forschungszentrum, "Basic Data for Modelling of Electrical Discharges in Gases: Oxygen", Tech. Note KLR 86-11C (1986).
- [6] R.F. Hampson, "Chemical Kinetic and Photochemical Data Sheets for Atmospheric Reactions", U.S. Dept. Transportation, Rep. No. FAA-EE-80-17 (1980).
- [7] J.S. Chang, R.M. Hobson, Y. Ichikawa, T. Kaneda, "Atomic and Molecule Processes in an Ionized Gas", Tokyo Denki University press, Tokyo (1983).
- [8] Y. Ichikawa and S. Teii, *J. Phys. D: Appl. Phys.*, **13**, 2031 (1980).
- [9] T. Kaneda, Y. Ichikawa, R.L.C. Wu and T.O. Tiernan, *Tokyo Denki University Eng. Res. Rep.*, **31**, 17 (1983).
- [10] J.S. Chang, *Proc. 17th Int. Conf. Phenomena in Ionized Gases*; **1**, pp. 45-48 (1985).
- [11] D. Rapp, P. Englander-Golden and D.D. Briglia, *J. Chem. Phys.*, **42**, 4081 (1985).
- [12] B. Evans, S. Ono, R.M. Hobson, S. Teii, A.W. Yau and J.S. Chang, *Shock Tubes and Waves*, C. Treanor and J. Gordon Hall, Eds., SUNY Press, NY, pp. 535-542 (1982).
- [13] D. Spence and G.J. Schulz, *Phys. Rev. A*, **A5**, 724 (1972).
- [14] S. Ono, J.S. Chang and S. Teii, to be published (1987).